Supporting Information for:

Mechanistic investigations of the formation of highly oxidized products from the multi-generation OH oxidation of styrene

Long Chen,[1,2,3] Yu Huang,*[1,2,3] Yonggang Xue,[1,2,3] Long Cui,[1,2,3] Zhihui Jia[4]

[1] *State Key Laboratory of Loess Science, Institute of Earth Environment, Chinese Academy of Sciences, Xi'an 710061, China*

[2] *National Observation and Research Station of Regional Ecological Environment Change and Comprehensive Management in the Guanzhong Plain, Xi'an 710061, China*

[3] *Shaanxi Key Laboratory of Atmospheric and Haze-fog Pollution Prevention, Xi'an 710061, China*

[4] *School of Materials Science and Engineering, Shaanxi Normal University, Xi'an, Shaanxi, 710119, China*

Submitted to *Atmospheric Chemistry & Physics*

*Corresponding author:
Prof. Yu Huang, E-mail address: huangyu@ieecas.cn

Table S1 The relative electronic energy (ΔE_i), free energy (ΔG_i) and Boltzmann population (w_i) of different conformers involved in S2-1-x predicted at the M06-2X/6-311++G(3df,3pd)//M06-2X/6-31+G(d,p) level

Conformer	ΔE_i(kcal/mol)	ΔG_i(kcal/mol)	w_i
S2-1-a	0.00	0.00	57.32%
S2-1-b	0.18	0.36	31.21%
S2-1-c	1.34	1.08	9.25%
S2-1-d	2.58	2.51	0.83%
S2-1-e	2.87	2.88	0.44%
S2-1-f	2.98	3.18	0.27%
S2-1-g	3.58	2.86	0.46%
S2-1-h	3.60	3.27	0.23%

Table S2 The relative electronic energy (ΔE_i), free energy (ΔG_i) and Boltzmann population (w_i) of different conformers involved in S8-x predicted at the M06-2X/6-311++G(3df,3pd)//M06-2X/6-31+G(d,p) level

Conformer	ΔE_i(kcal/mol)	ΔG_i(kcal/mol)	w_i
S8-a	0.00	0.00	85.78%
S8-b	1.27	1.20	11.30%
S8-c	1.75	2.43	1.42%
S8-d	2.44	2.58	1.10%
S8-e	2.86	3.18	0.40%

Table S3 The activation energy (ΔE_a), IRC-TST rate coefficient ($k_{IRC\text{-}TST}$), Boltzmann populations (w_i) of conformer *i*, and MC-TST rate coefficient ($k_{MC\text{-}TST}$) calculated at the M06-2X/6-311++G(3df,3pd)//M06-2X/6-31+G(d,p) level

Reactions	ΔE_a(kcal/mol)	$k_{IRC\text{-}TST}$ (s^{-1})	w_i	$k_{MC\text{-}TST}$(s^{-1})
S8-a → S8-a-P	24.3	4.3×10^{-4}	85.78%	8.2×10^{9}
S8-b → S8-b-P	8.4	3.1×10^{6}	11.30%	
S8-c → S8-c-P	0.6	5.8×10^{11}	1.42%	
S8-d → S8-d-P	34.2	7.2×10^{-10}	1.10%	
S8-e → S8-e-P	11.8	5.4×10^{4}	0.40%	

Table S4 The relative electronic energy (ΔE_i), free energy (ΔG_i) and Boltzmann population (w_i) of different conformers involved in S28-x predicted at the M06-2X/6-311++G(3df,3pd)//M06-2X/6-31+G(d,p) level

Conformer	ΔE_i(kcal/mol)	ΔG_i(kcal/mol)	w_i
S28-a	0.00	0.00	88.79%
S28-b	1.50	1.41	8.21%
S28-c	1.97	2.11	2.52%
S28-d	3.88	3.14	0.44%
S28-e	4.49	4.42	0.05%

Table S5 The activation energy (ΔE_a), IRC-TST rate coefficient ($k_{IRC\text{-}TST}$), Boltzmann populations (w_i) of conformer *i*, and MC-TST rate coefficient ($k_{MC\text{-}TST}$) calculated at the M06-2X/6-311++G(3df,3pd)//M06-2X/6-31+G(d,p) level

Reactions	ΔE_a(kcal/mol)	$k_{IRC\text{-}TST}$ (s^{-1})	w_i	$k_{MC\text{-}TST}$(s^{-1})
S28-a → S28-a-P	12.7	8.9×10^{4}	88.79%	1.7×10^{9}
S28-b → S28-b-P	25.6	6.2×10^{-4}	8.21%	
S28-c → S28-c-P	38.3	7.3×10^{-12}	2.52%	
S28-d → S28-d-P	6.0	5.1×10^{7}	0.44%	
S28-e → S28-e-P	2.0	3.4×10^{10}	0.05%	

Table S6 Predicted saturated vapour pressure (P^0) and saturated concentrations (c^0) of styrene and its multiple generation oxidation closed-shell products

	Species	P^0 (atm)	c^0 (ug/m^3)	Species	P^0 (atm)	c^0 (ug/m^3)
Initial reactant	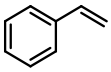 Styrene (C_8H_8)	4.63×10^{-3}	1.95×10^{7}			
First generation products	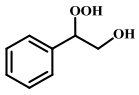 S4 ($C_8H_{10}O_3$)	1.43×10^{-7}	8.89×10^{2}	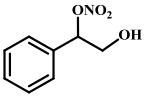 S5 ($C_8H_9NO_3$)	2.54×10^{-7}	1.87×10^{3}
	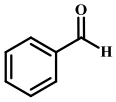 Benzaldehyde (C_7H_6O)	7.62×10^{-4}	2.89×10^{6}			
Second generation products	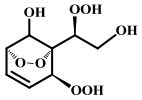 S6 ($C_8H_{12}O_8$)	4.72×10^{-12}	4.50×10^{-2}	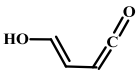 S10 ($C_4H_4O_2$)	6.41×10^{-4}	2.17×10^{6}
	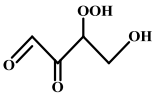 S12 ($C_4H_6O_5$)	1.83×10^{-7}	9.91×10^{2}	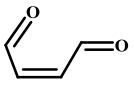 S14 ($C_4H_4O_2$)	2.48×10^{-3}	8.39×10^{6}
	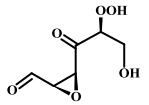 S20 ($C_6H_8O_6$)	5.11×10^{-9}	42.21	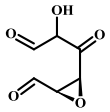 S23 ($C_6H_6O_5$)	6.73×10^{-8}	4.31×10^{2}
	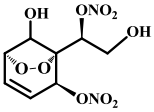 S26 ($C_8H_{10}N_2O_{10}$)	1.52×10^{-11}	0.18	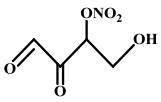 S32 ($C_4H_5NO_6$)	3.29×10^{-7}	2.16×10^{3}

Third generation products	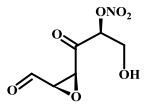 S40-1 ($C_6H_7NO_7$)	9.16×10^{-9}	75.86			
	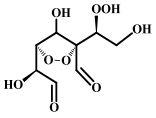 S47 ($C_8H_{12}O_9$)	2.64×10^{-14}	2.68×10^{-4}	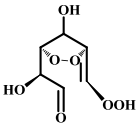 S48 ($C_6H_8O_7$)	4.63×10^{-10}	3.59
	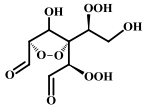 S51($C_8H_{12}O_{10}$)	1.46×10^{-14}	1.58×10^{-4}	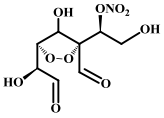 S58 ($C_8H_{11}NO_{10}$)	4.73×10^{-14}	5.37×10^{-4}
	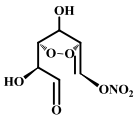 S59 ($C_6H_7NO_8$)	1.14×10^{-9}	10.16	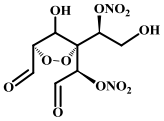 S62 ($C_8H_{10}N_2O_{12}$)	4.70×10^{-14}	6.18×10^{-4}

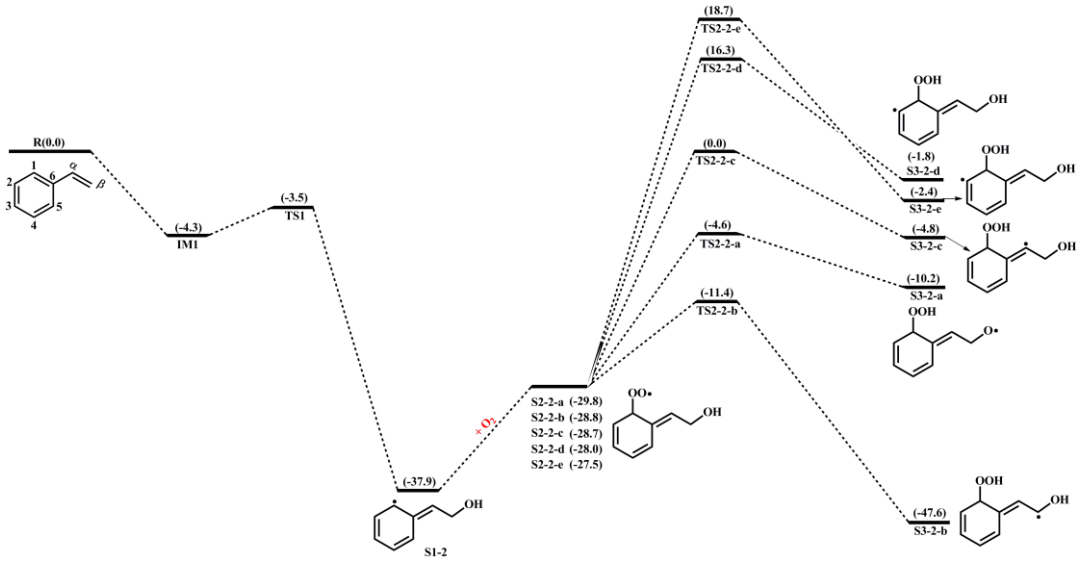

Figure S1. PES for the OH-initiated oxidation of styrene and the unimolecular reactions of S2-2-x at the M06-2X/6-311++G(3df,3pd)//M06-2X/6-31+g(d,p) level

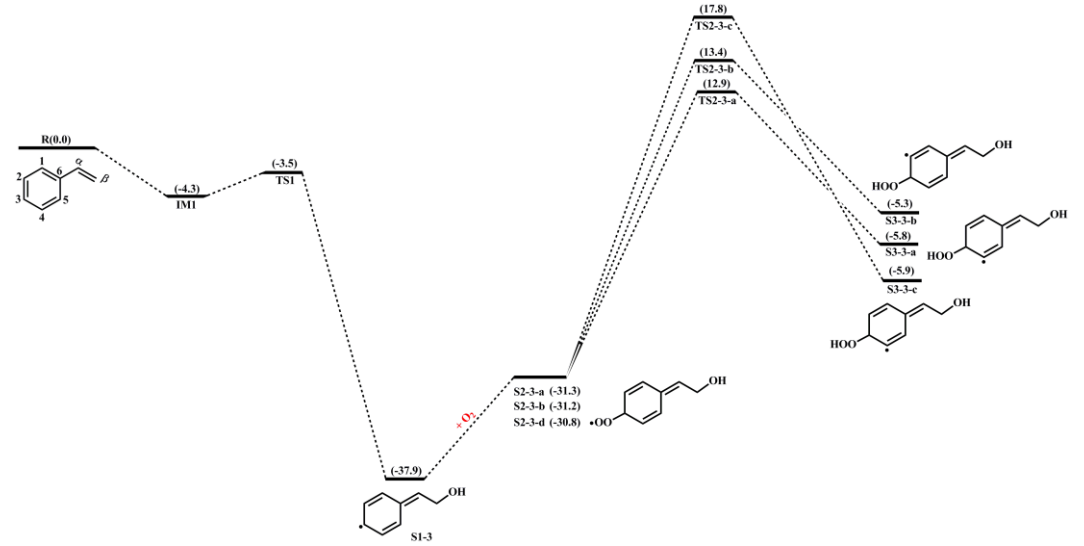

Figure S2. PES for the OH-initiated oxidation of styrene and the unimolecular reactions of S2-3-x at the M06-2X/6-311++G(3df,3pd)//M06-2X/6-31+g(d,p) level

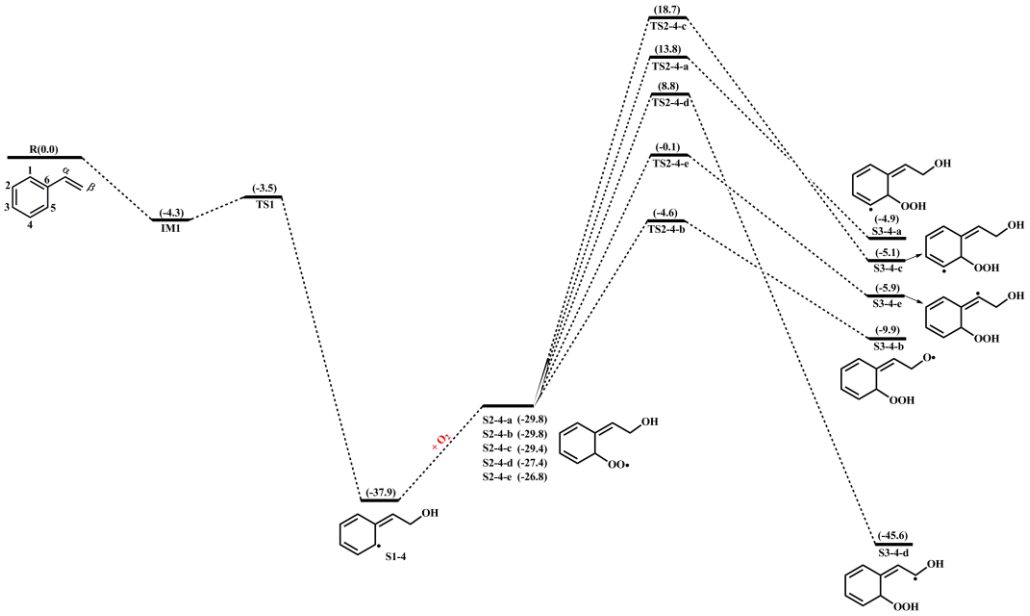

Figure S3. PES for the OH-initiated oxidation of styrene and the unimolecular reactions of S2-4-x at the M06-2X/6-311++G(3df,3pd)//M06-2X/6-31+g(d,p) level

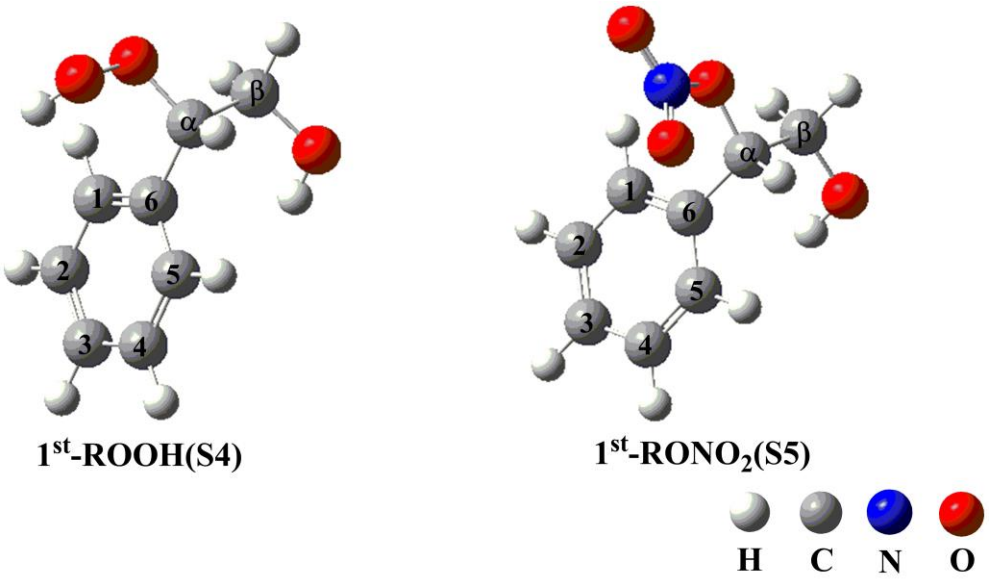

Figure S4. Global minimum structures of 1st-ROOH(S4) and 1st-$RONO_2$(S5) at the M06-2X/6-31+g(d,p) level

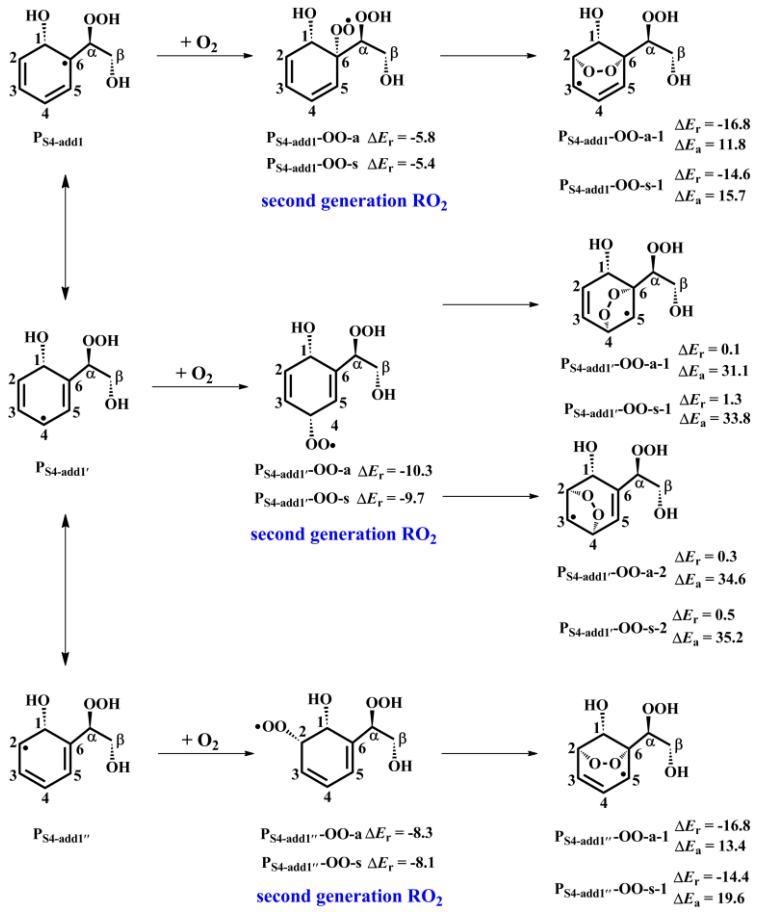

Figure S5. PES for the addition reactions $P_{S4\text{-}add1}$ + O_2 and subsequent intramolecular cyclization reactions at the M06-2X/6-311++G(3df,3pd)//M06-2X/6-31+g(d,p) level (the symbols s and a represent *syn*- and *anti*-O_2-addition)

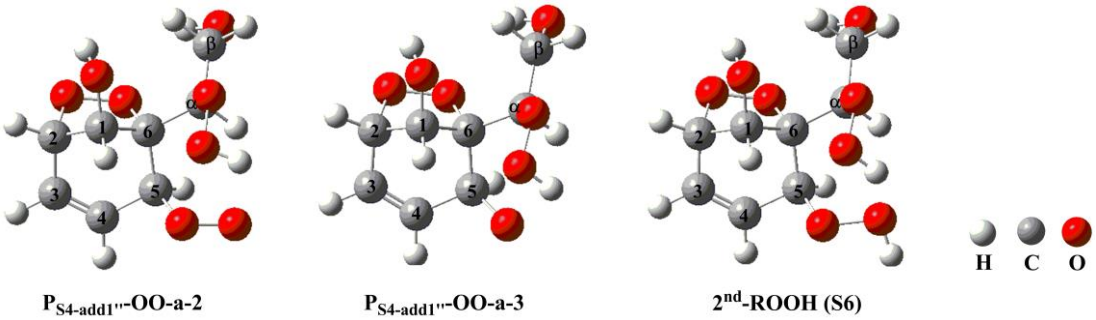

Figure S6. The lowest energy conformers of third generation peroxy radical $P_{S4\text{-}add1''}$-OO-a-2, $P_{S4\text{-}add1''}$-OO-a-3 and 2^{nd}-ROOH(S6) at the M06-2X/6-31+g(d,p) level

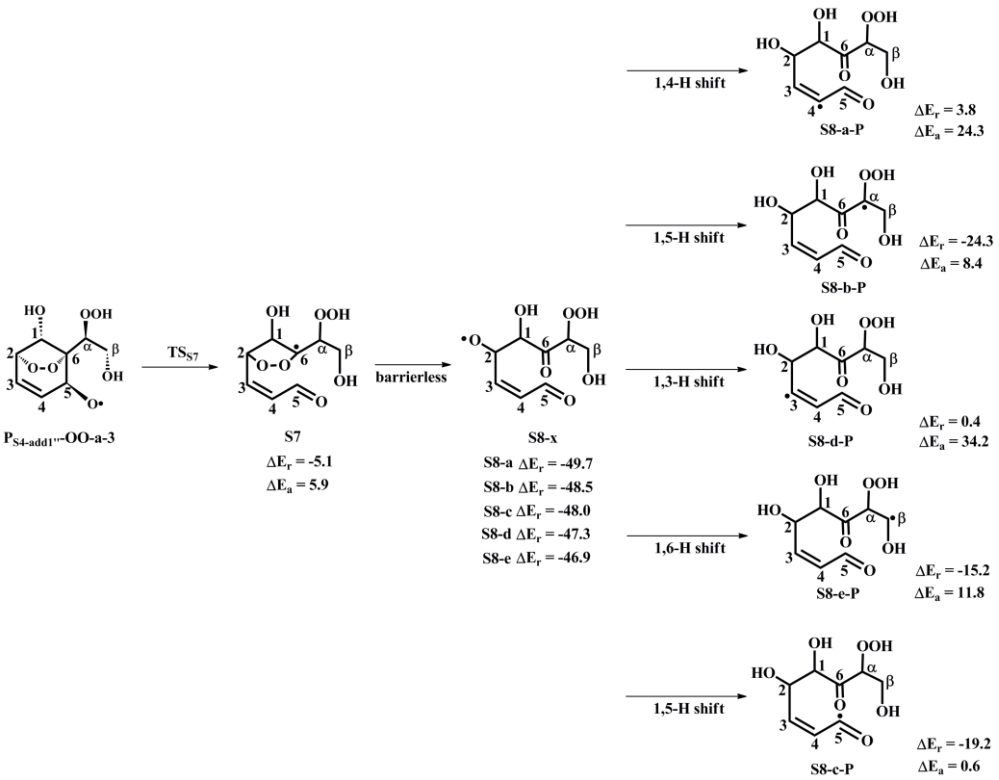

Figure S7. PES for the intramolecular hydrogen transfer reactions of S8-x at the M06-2X/6-31+g(d,p) level

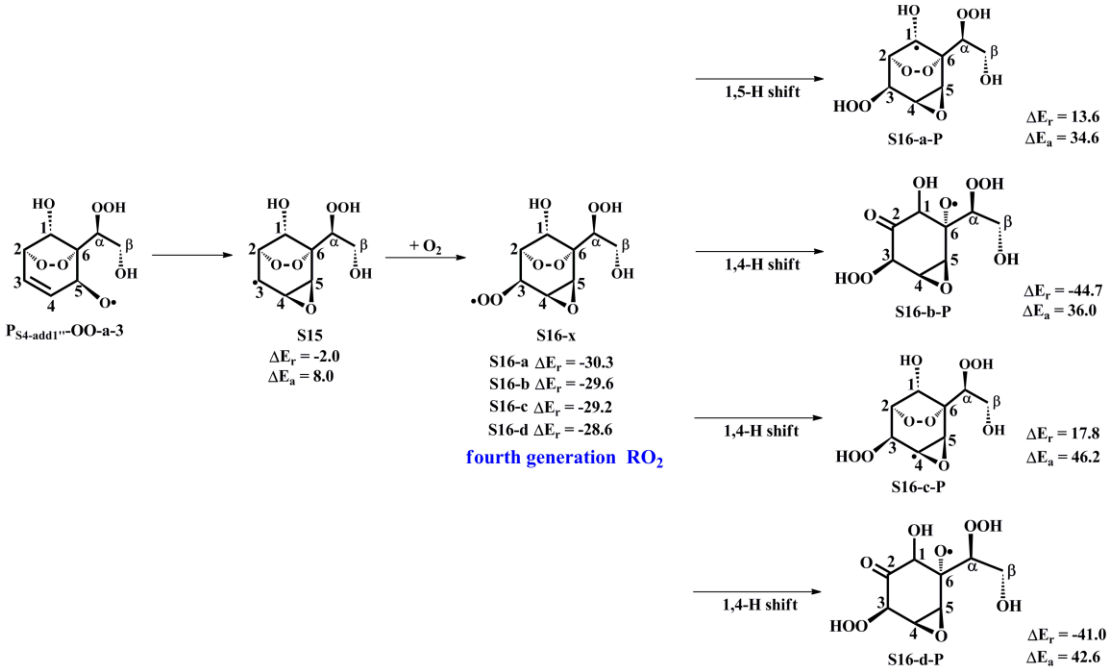

Figure S8. PES for the intramolecular hydrogen transfer reactions of S16-x at the M06-2X/6-31+g(d,p) level

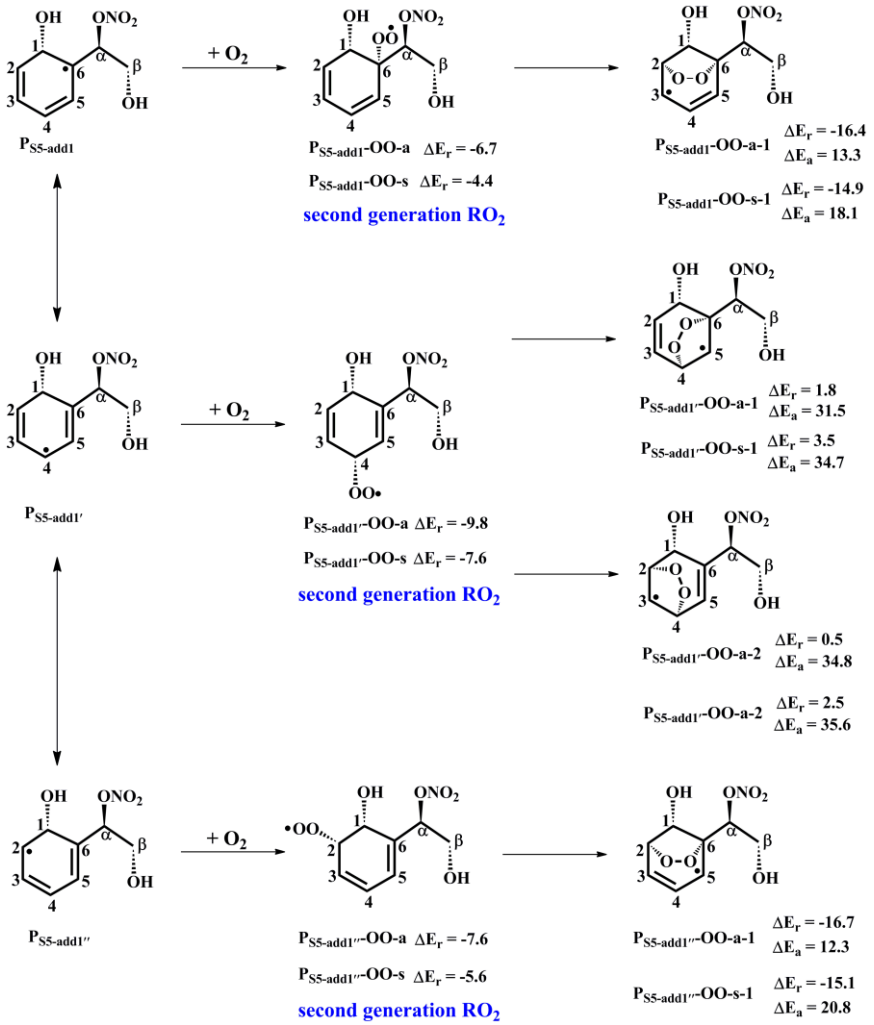

Figure S9. PES for the addition reactions $P_{S5\text{-}add1}$ + O_2 and subsequent cyclization reactions at the M06-2X/6-311++G(3df,3pd)//M06-2X/6-31+g(d,p) level (the symbols s and a represent *syn*- and *anti*-O_2-addition)

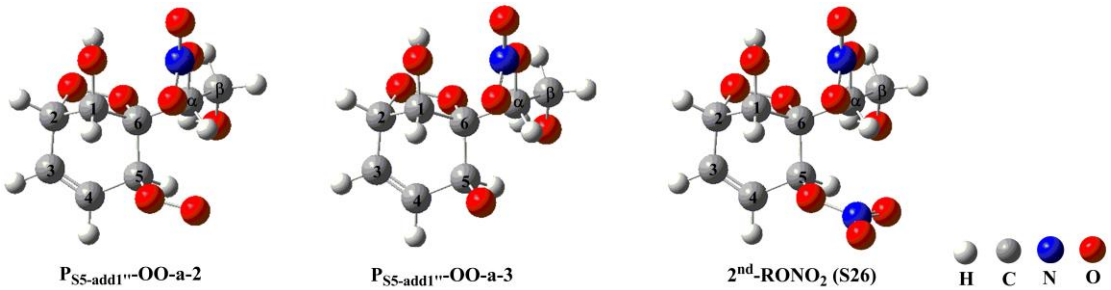

Figure S10. The lowest energy conformers of third generation peroxy radical $P_{S5\text{-}add1''}$-OO-a-2, $P_{S5\text{-}add1''}$-OO-a-3 and 2^{nd}-$RONO_2$(S26) at the M06-2X/6-31+g(d,p) level

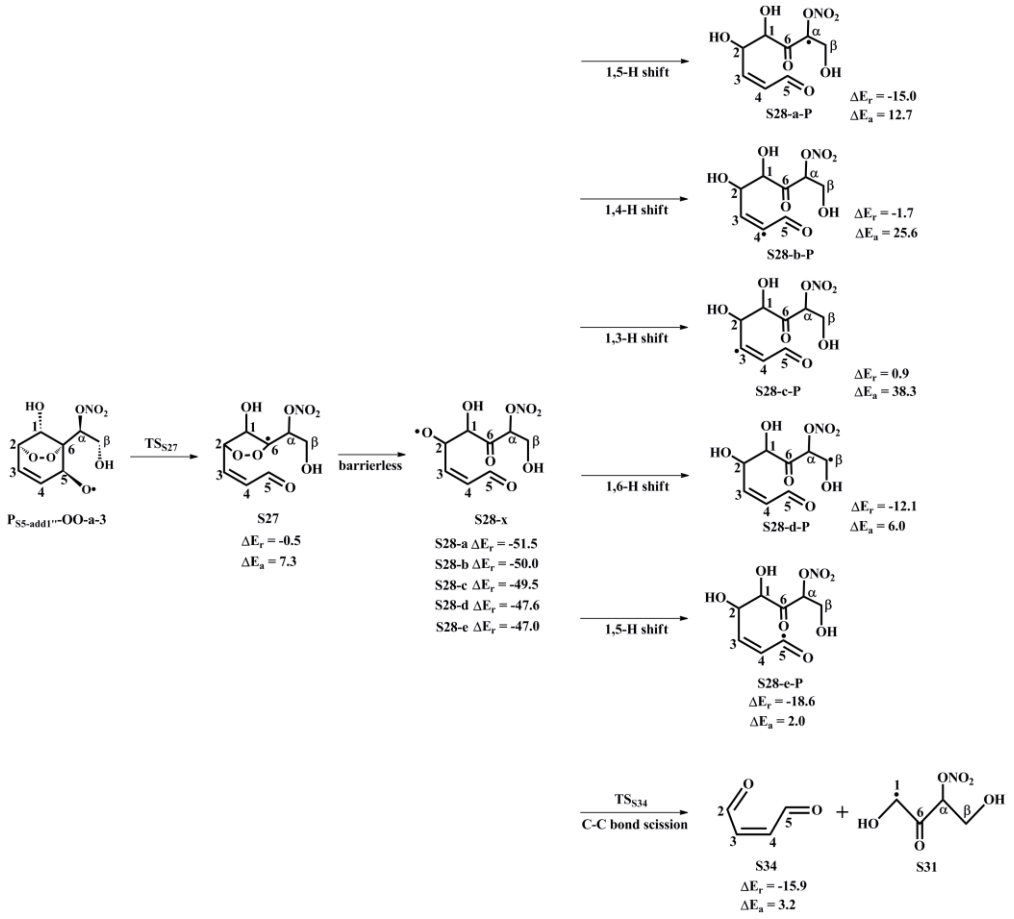

Figure S11. PES for the intramolecular hydrogen transfer reactions of S28-x at the M06-2X/6-311++G(3df,3pd)//M06-2X/6-31+g(d,p) level

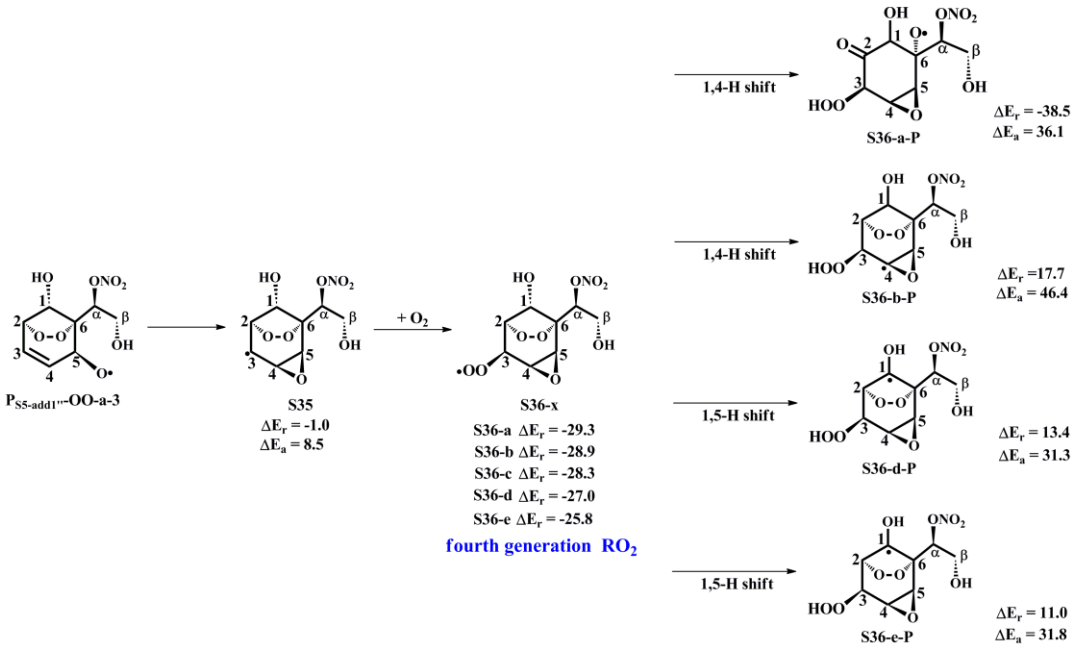

Figure S12. PES for the intramolecular hydrogen transfer reactions of S36-x at the M06-2X/6-311++G(3df,3pd)//M06-2X/6-31+g(d,p) level

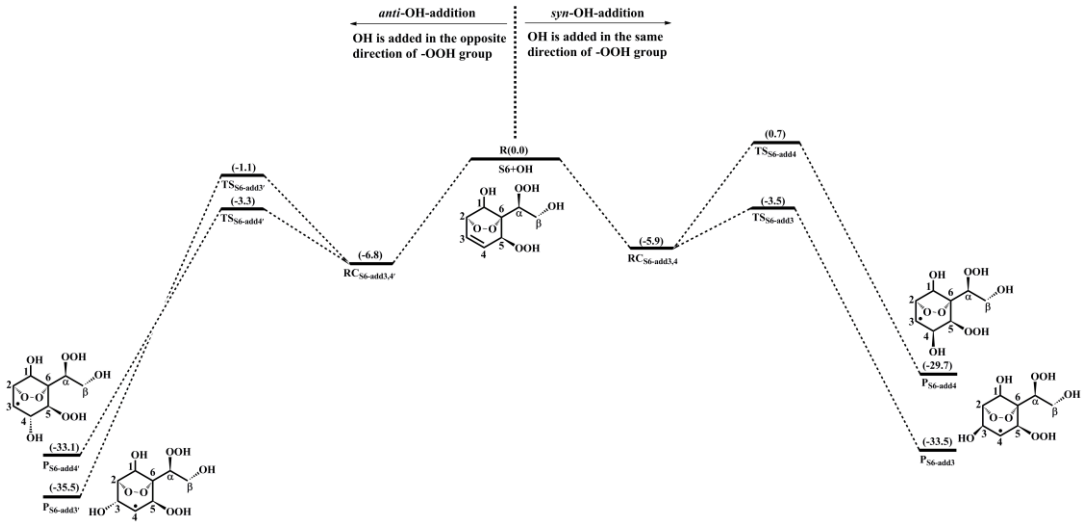

Figure S13. PES for the oxidation of 2[nd]-ROOH (S6) initiated by OH radicals at the M06-2X/6-311++G(3df,3pd)//M06-2X/6-31+g(d,p) level

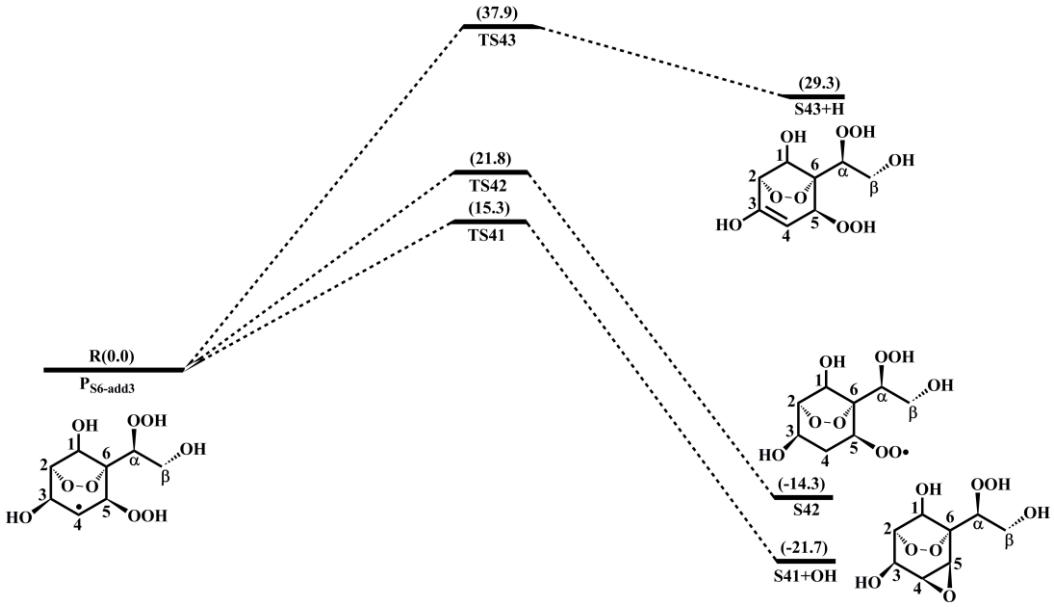

Figure S14. PES for the unimolecular decomposition of $P_{S6\text{-}add3}$ at the M06-2X/6-311++G(3df,3pd)//M06-2X/6-31+g(d,p) level

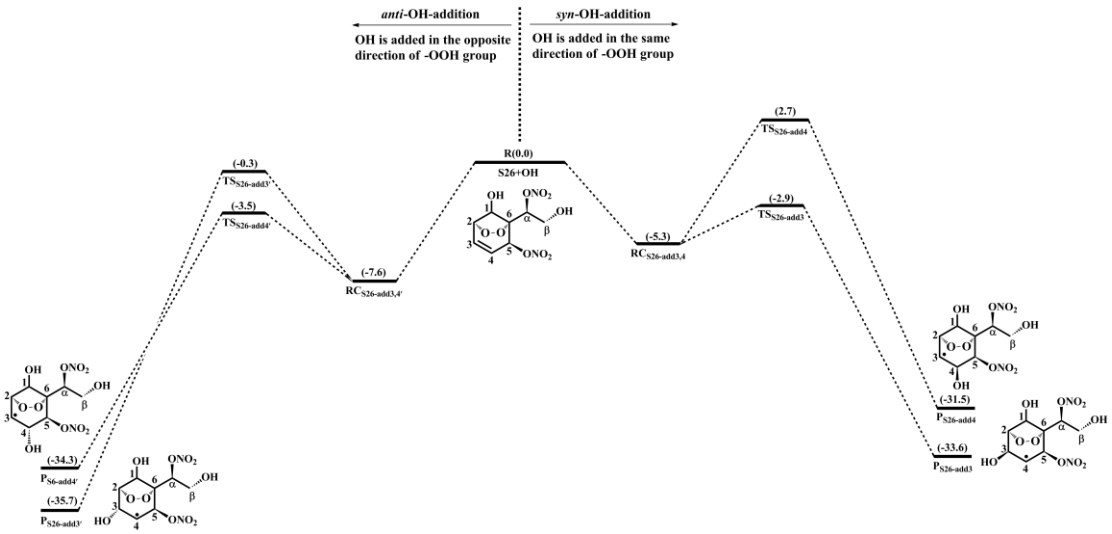

Figure S15. PES for the oxidation of 2^{nd}-$RONO_2$ (S26) initiated by OH radicals at the M06-2X/6-311++G(3df,3pd)//M06-2X/6-31+g(d,p) level

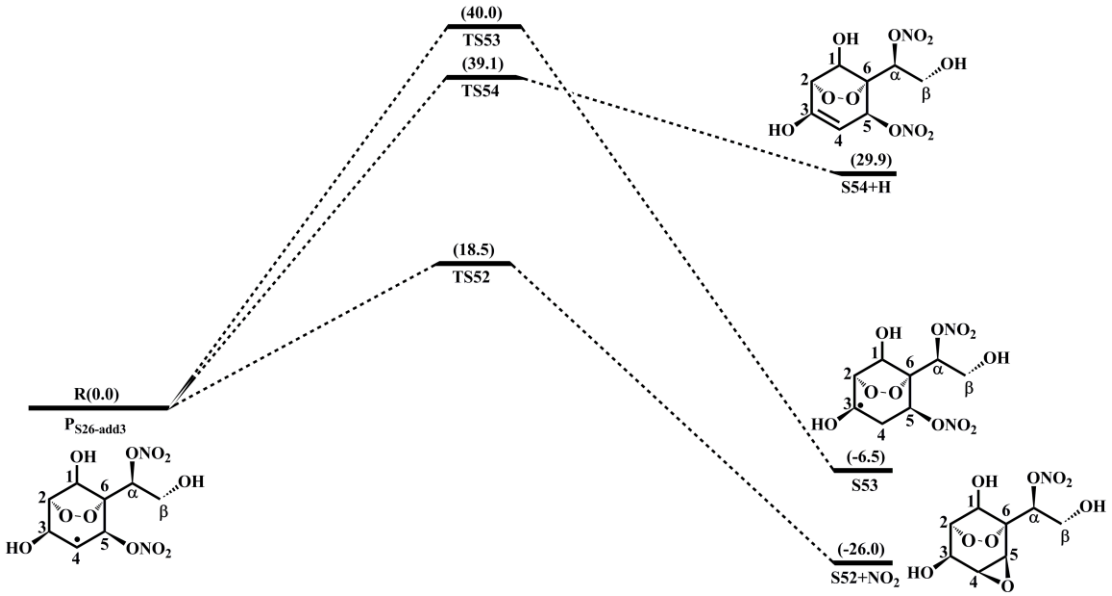

Figure S16. PES for the unimolecular decomposition of $P_{S26\text{-}add3}$ at the M06-2X/6-311++G(3df,3pd)//M06-2X/6-31+g(d,p) level